



Mechanism and modelling of thermally initiated RAFT step-growth polymerization

Journal:	<i>Polymer Chemistry</i>
Manuscript ID	PY-COM-10-2024-001188.R2
Article Type:	Communication
Date Submitted by the Author:	03-Dec-2024
Complete List of Authors:	Clouthier, Samantha; University of North Carolina at Chapel Hill Campus Box 3290 Chapel Hill, NC 27599-3290, USA , Department of Chemistry Tanaka, Joji; University of North Carolina at Chapel Hill, You, Wei; The University of North Carolina at Chapel Hill, Chemistry

COMMUNICATION

Mechanism and modelling of thermally initiated RAFT step-growth polymerization

Samantha Marie Clouthier,^a Joji Tanaka^{a*} and Wei You^{a*}

Received 00th January 20xx,
Accepted 00th January 20xx

DOI: 10.1039/x0xx00000x

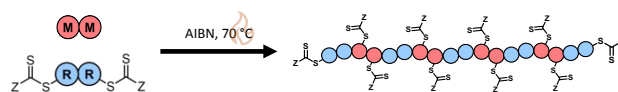
Here we report the modelling of thermally initiated RAFT step-growth polymerization kinetics of maleimide and acrylate monomers with bifunctional RAFT agents bearing tertiary carboxyalkyl stabilized fragmentable R groups. By analytically solving the governing equations of our model as derived from the proposed mechanism, we demonstrate that the kinetics for these polymerizations follows first order with respect to monomer concentration. Furthermore, the obtained apparent rate constant (k_{app}) values indicate that acrylate monomers polymerize at slow rates compared to maleimide monomers during thermally initiated RAFT step-growth polymerization.

Reversible addition fragmentation chain transfer (RAFT) is a controlled radical polymerization (CRP) technique mediated by chain transfer agents (CTA, or RAFT agents) that proceeds by a degenerative chain transfer mechanism.¹⁻⁶ Although RAFT polymerizations are considered advantageous due to the user-friendly nature of the polymerization, high functional group tolerance, and ability to polymerize a wide range of monomer classes, RAFT is predominantly limited to all carbon backbones.³ Step-growth polymerizations on the other hand involves the reaction of two functional groups to form polymers in a step wise manner. As such, a wide range of backbone functionalities can be incorporated into the monomer utilized for polymerization. However, step-growth polymerizations often require harsh conditions to achieve sufficient monomer conversion and high molecular weight polymers,⁷ which limits the functionalities that can be incorporated into the backbone.

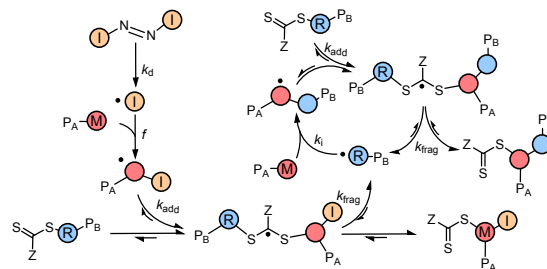
RAFT step-growth polymerization combines the beneficial characteristics of RAFT polymerization, like the user-friendly nature and high functional group tolerance, with the versatility in backbone functionality from step growth-polymerization, giving access to highly functional polymer backbones (Scheme 1A).⁸⁻¹³ As such, RAFT

Scheme 1: (A) General RAFT step-growth polymerization scheme. (B) Thermally initiated RAFT step-growth mechanism.

A General Polymerization Scheme



B RAFT Step-Growth Polymerization Initiated by AIBN



step-growth polymerization provides a route to functional polymer backbones with foreseeable applications from drug delivery to chemical recycling.^{13, 14}

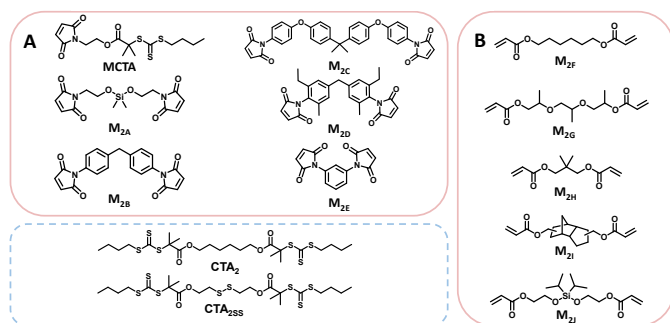
RAFT step-growth typically employs bifunctional reagents for both monomer and CTA and proceeds through a single unit monomer insertion (SUMI) mechanism (Scheme 1). The basics of the RAFT-SUMI mechanism and kinetics have been explored in previous investigations, including effect of monomer¹⁵⁻¹⁷ and initiation method.¹⁸ As shown below, RAFT step-growth traditionally proceeds by the thermal decomposition of exogenous azo-initiator to generate the radicals used in the RAFT step-growth cycle, similar to thiol-ene step-growth polymerization (Scheme 1B).¹⁹⁻²¹ The RAFT step-growth cycle can be broken down into three steps: (1) monomer addition to CTA derived R^\bullet radical to generate a monomer (or backbone) derived M^\bullet radical (k_i , Scheme 1B), (2) RAFT agent addition to M^\bullet radical to generate a chain transfer intermediate radical adduct CTA^\bullet (k_{add} , Scheme 1B), and (3) fragmentation of CTA^\bullet to regenerate the CTA

^a Department of Chemistry, University of North Carolina at Chapel Hill, Chapel Hill, NC 27599-3290 (USA). E-mail: joji@email.unc.edu, wyou@unc.edu.

* Footnotes relating to the title and/or authors should appear here.

Electronic Supplementary Information (ESI) available: [details of any supplementary information available should be included here]. See DOI: 10.1039/x0xx00000x

Scheme 2: Monomers discussed in this work



derived R^\bullet radical (k_{frag} , **Scheme 1B**). The driving force for the polymerization to proceed through by step-growth over chain-growth is driven by low homopropagation (k_p), high k_i and high chain transfer equilibrium described by ratio of forward and reverse chain transfer constant coefficient (C_{tr}/C_{tr}).¹³

Thermally initiated RAFT step-growth has been demonstrated with both maleimides (MCTA-M_{2E}) and acrylates (M_{2F}-M_{2J}) monomers with bifunctional RAFT agents that bear tertiary carboxyalkyl R groups (MCTA, CTA₂, and CTA_{2SS}) (**Scheme 2**).⁸⁻¹⁰ Thus far, kinetics of RAFT step-growth polymerizations has been treated as pseudo-first order reactions *without* consideration to the rate limiting steps.⁸⁻¹⁰ Here, we investigate the mechanism of thermally initiated RAFT step-growth of maleimide and acrylate monomers through kinetic modelling, where we consider rate limiting steps of the RAFT step-growth cycle and subsequently fit experimental data following our kinetic models to obtain apparent rate constants (k_{app}).

To aid the interpretation of the observed polymerization kinetics for thermally initiated RAFT step-growth, we have developed a model based on the key steps in the mechanism. The model is based on the proposed mechanism (**Scheme 1B**) involving 5 species: the monomer (M), RAFT agent (CTA), as well as three radical species generated by the cycle (backbone radical (M \bullet), RAFT agent radical (R \bullet), and RAFT step-growth adduct radical (CTA \bullet). From these species, we defined governing equations for the model (equations 1-5), where equations 1 and 2 describe the consumption of monomer groups by monomer addition to R \bullet and consumption of RAFT agent by addition, respectively. Equations 1 and 2 assume that consumption of monomer or RAFT agent groups by initiation is negligible. Additionally, equations 3-5 describe the concentrations of the three radical species in the RAFT step-growth cycle, accounting for initiation (in the case of equation 3), termination, and generation and consumption throughout the RAFT step-growth cycle. For simplification, the reverse chain transfer process in the RAFT step-growth cycle is not considered. This is a reasonable assumption, particularly for examples where the CTA bearing a more radically stabilized fragmentable group (R \bullet) relative to monomer derived radical species (M \bullet).

$$\frac{d[M]}{dt} = -k_i[M][R^\bullet]$$

$$\frac{d[CTA]}{dt} = -k_{add}[CTA][M^\bullet] \quad (1)$$

(2)

$$\frac{d[M^\bullet]}{dt} = R_i - R_t(R^\bullet) + k_i[M][R^\bullet] - k_{add}[CTA][M^\bullet] \quad (3)$$

$$\frac{d[R^\bullet]}{dt} = -R_t(R^\bullet) - k_i[M][R^\bullet] + k_{frag}[CTA^\bullet] \quad (4)$$

$$\frac{d[CTA^\bullet]}{dt} = -R_t(CTA^\bullet) - k_{frag}[CTA^\bullet] + k_{add}[CTA][M^\bullet] \quad (5)$$

The initiation rate (R_i) accounted for in equation 3 is defined by equation 6, where f is the initiation efficiency of monomer adding to the initiator radical (I^\bullet), k_d is the decomposition rate of the initiator, and $[I]$ is the concentration of initiator species. Notably, defining R_i in this manner has limitation at high monomer conversion due to the assumption of a constant value for f . Because of radical side reactions, a value of $f = 1$ is not recommended; rather, a value of $f = 0.65$ has been recommended and adopted for azo-initiators.^{13, 22} Nevertheless, initiator efficiency (f) is expected to fall at high monomer conversion (when monomer concentration becomes a limiting factor). Rates of termination ($R_t(M^\bullet)$, $R_t(R^\bullet)$, and $R_t(CTA^\bullet)$) by a variety of radical-radical combination events are highlighted below in equations 7-9. Notably, all termination events by radical-radical combination are assumed to be equally likely, thus termination related rate constants (k_{t1} , k_{t2} , k_{t3} , k_{t4} , k_{t5} , and k_{t6}) are all equal and can be further simplified by a general termination kinetic parameter (k_t). Furthermore, equations 7-9 can be summed together to give a general rate of termination (R_t) (equation 10).

$$R_i = 2fk_d[I] \quad (6)$$

$$R_t(M^\bullet) = 2k_{t1}[M^\bullet]^2 + k_{t2}[M^\bullet][R^\bullet] + k_{t3}[M^\bullet][CTA^\bullet] \quad (7)$$

$$R_t(R^\bullet) = k_{t2}[M^\bullet][R^\bullet] + 2k_{t4}[R^\bullet]^2 + k_{t5}[R^\bullet][CTA^\bullet] \quad (8)$$

(9)

(10)

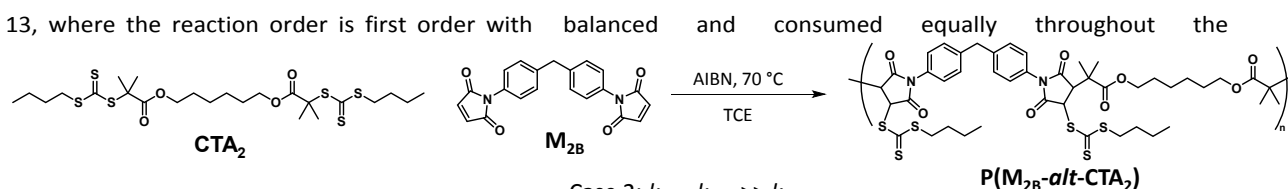
$$R_t(CTA^\bullet) = k_{t3}[M^\bullet][CTA^\bullet] + k_{t5}[R^\bullet][CTA^\bullet] + 2k_{t6}[CTA^\bullet]^2$$

$$R_t = R_t(M^\bullet) + R_t(R^\bullet) + R_t(CTA^\bullet)$$

The rate of polymerization (R_p) can be analytically solved using equations 1-10. Consumption rates of monomer and RAFT agent can be assumed to be equal, and therefore, equations 1 and 2 can be set equal. Furthermore, the steady state approximation can be adopted, allowing for equations 3-5 to be set equal to zero, giving equation 11 as the overall rate expression (see SI for a more detailed derivation of equation 11).

Equation 11 can be simplified by establishing various limiting cases between the three kinetic parameters of the RAFT step-growth cycle (k_{frag} , k_i , and k_{add}). In case 1, the fragmentation of the RAFT step-growth radical adduct is established as the rate limiting step (k_{add} , $k_i \gg k_{frag}$), which gives equation 12 and establishes RAFT step-growth as a zeroth order reaction. Case 2 assumes that the monomer addition to R \bullet species is rate limiting (k_{add} , $k_{frag} \gg k_i$), simplifying the R_p term

to equation 13, where the reaction order is first order with respect to monomer concentration. Additionally, case 3 can be

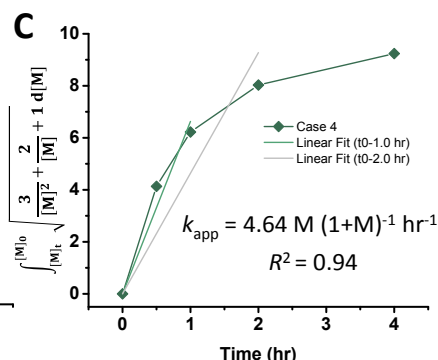
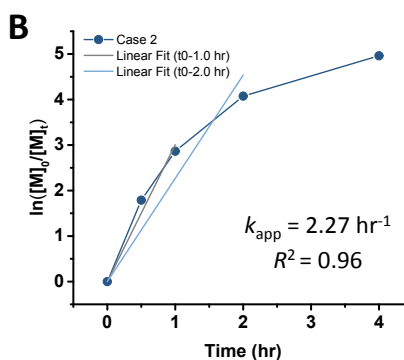
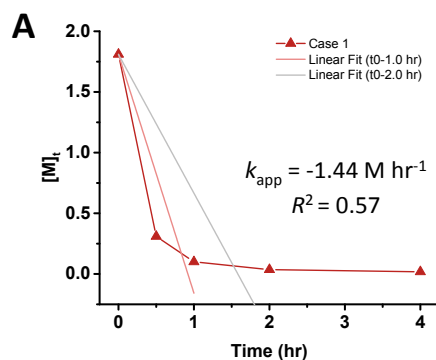


Case 1: $k_{\text{add}}, k_i \gg k_{\text{frag}}$

Case 2: $k_{\text{add}}, k_{\text{frag}} \gg k_i$

Case 3: $k_i, k_{\text{frag}} \gg k_{\text{add}}$

Case 4: $k_{\text{frag}} \approx k_{\text{add}} \approx k_i$



monomer concentration. Additionally, case 3 can be

polymerization.

Case 1: $k_{\text{add}}, k_i \gg k_{\text{frag}}$

$$(12) \quad R_p = \frac{d[M]}{dt} = \sqrt{\frac{fk_d[I]}{k_t}} (k_{\text{frag}})$$

Case 2: $k_{\text{add}}, k_{\text{frag}} \gg k_i$

$$(13) \quad R_p = \frac{d[M]}{dt} = \sqrt{\frac{fk_d[I]}{k_t}} (k_i[M])$$

Case 3: $k_{\text{frag}}, k_i \gg k_{\text{add}}$

$$(14) \quad R_p = \frac{d[M]}{dt} = \sqrt{\frac{fk_d[I]}{k_t}} (k_{\text{add}}[M])$$

$$R_p = \frac{d[M]}{dt} = \sqrt{\frac{R_i}{2k_t}} \frac{1}{\sqrt{\frac{1}{(k_{\text{add}}[CTA])^2} + \frac{1}{k_i[M]k_{\text{add}}[CTA]} + \frac{1}{k_{\text{add}}[CTA]k_{\text{frag}}} + \frac{1}{(k_i[M])^2} + \frac{1}{k_i[M]k_{\text{frag}}} + \frac{1}{(k_{\text{frag}})^2}}}}$$

(11)

defined by establishing end-group RAFT agent addition to backbone radical M^\bullet as the rate limiting step ($k_{\text{frag}}, k_i \gg k_{\text{add}}$), giving equation 14 as the simplified R_p term. Case 3 also demonstrates first order dependence with respect to monomer concentration. Lastly for case 4, all kinetic parameters are assumed to be approximately equal ($k_{\text{frag}} \approx k_{\text{add}} \approx k_i$) and defined as k_{case4} (i.e., $k_{\text{frag}} \approx k_{\text{add}} \approx k_i = k_{\text{case4}}$, equation 15). Note, monomer and RAFT agent concentrations are set equal ($[M] = [CTA]$) as they are assumed to be stoichiometrically

Case 4: $k_{\text{frag}} \approx k_{\text{add}} \approx k_i$

$$R_p = \frac{d[M]}{dt} = \sqrt{\frac{fk_d[I]}{k_t}} \frac{k_{\text{case4}}}{\sqrt{\left(\frac{3}{[M]^2} + \frac{2}{[M]} + 1\right)}} \quad (15)$$

Experimental polymerization data for maleimide and acrylate

Figure 1: Kinetic analysis of RAFT step-growth for maleimide monomers with monomer M_{2B} serving as a model monomer for fittings of various cases: (A) Case 1, where k_{frag} is the rate limiting step, (B) Cases 2 and 3, where either k_{add} or k_i are the rate limiting steps, and (C) Case 4, where all rate constants are equal.

monomers (**Scheme 2**) can be fit using the model predictions established from cases 1-4. As a result, experimental data of RAFT step-growth polymerization of CTA₂ and *N,N'*-(1,4-phenylene)dimalimide, M_{2B} (**Scheme 2**),⁹ was plotted according to each of the 4 cases established previously with linear regressions applied from 0 to 1.0 hours and 0 to 2.0 hours (**Figure 1**, **Table S1**). It is important to note that rate orders often change as a reaction progresses due to shifts in the rate-limiting step or the influence of competing reactions. While the rate fittings presented here focus on the initial stages of polymerization, the later stages are arguably more critical for step-growth polymerizations, as high monomer conversions are essential to achieve high molecular weights. Nevertheless, determining the rate order and apparent rate constants (k_{app}) for RAFT step-growth polymerization provides valuable quantitative insights, particularly when comparing the two reported monomer classes. Additionally, it should be acknowledged that ¹H-NMR analysis at high monomer conversions ($p > 98\%$) may be prone to errors.

Fitting the data according to case 1 ($k_{add}, k_i \gg k_{frag}$) where a zeroth order relation with respect to monomer concentration is predicted, gives poor fits (k_{app} is 1.44 M hr⁻¹ and $R^2 < 0.6$, where k_{app} is defined in equation S10) (**Figure 1A**, **Table S1**). Furthermore, both cases 2 and 3 ($k_{add}, k_{frag} \gg k_i$ and $k_i, k_{frag} \gg k_{add}$, respectively) give first order relation with respect to monomer concentration, and therefore, fitting with a first order plot cannot distinguish the two cases. Nevertheless, the polymerization data appears to follow first order kinetics ($k_{app} = 2.27$ hr⁻¹ and $R^2 = 0.96$, where k_{app} for cases 2 and 3 are defined by equations S11 and S12, respectively) (**Figure 1B**, **Table S1**). Notably, the polymerization plateaus after 2.0 hours, which is likely a result of efficiency factor, f , falling at high monomer conversion.²² Additionally, this plateau in the kinetics at high monomer conversion could be attributed to an increasing occurrence of retardation (*vide infra*). Lastly, case 4 ($k_{frag} \approx k_{add} \approx k_i$) was also fitted, giving a k_{app} value of 4.64 M (1+M)⁻¹ hr⁻¹ and an R^2 value of 0.94, where k_{app} for case 4 is defined in equation S13 (**Figure 1C**, **Table S1**).

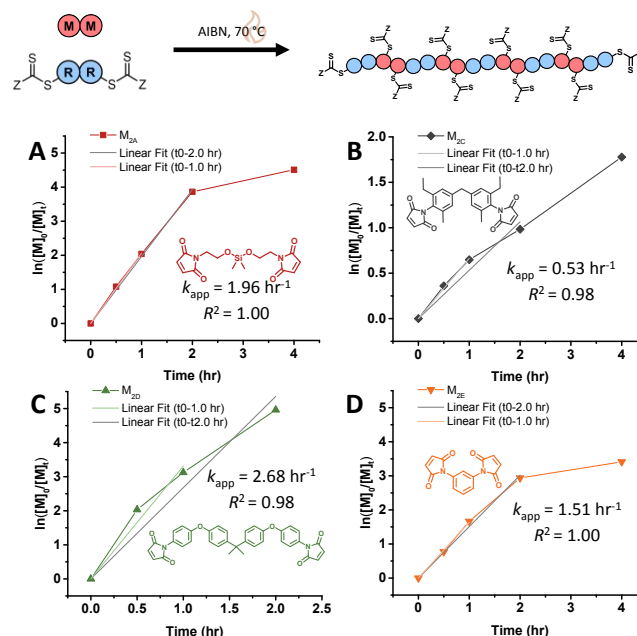


Figure 2: Kinetic analysis of RAFT step-growth for maleimide monomers with CTA₂: (A) M_{2A}, (B) M_{2C}, (C) M_{2D}, and (D) M_{2E}.

Similarly, the polymerization data of monomer 1,6-hexanediol diacrylate, M_{2F}, with CTA₂ (**Scheme 2**),¹⁰ can be plotted according to the same 4 cases as before with linear regressions from 0 to 4.0 hours (**Figure S1**, **Table S2**), where again cases 2 and 3 give the best fit ($k_{app} = 0.98$ hr⁻¹ $R^2 = 1.00$) compared to cases 1 and 4 (where $k_{app} = -0.29$ M hr⁻¹ and 1.87 M (1+M)⁻¹ hr⁻¹ and $R^2 = 0.82$ and 1.00, respectively). Notably, the polymerization kinetics for RAFT step-growth of acrylates does not demonstrate a plateau at high monomer conversion as observed in the case of maleimides (**Figure 2**), possibly indicating that the monomer addition to the initiator radical (which is accounted for by f) is less rate limiting for acrylates than maleimides.

As observed, case 2 and 3 yield the best linear fit for the experimental data; however, this alone does not distinguish between the two cases. Additionally, fitting case 4 results in only slightly lower R^2 values compared to cases 2 and 3, making it difficult to differentiate between these cases based solely on model fitting. Nonetheless, due to the reactive nature of the trithiocarbonate, it is unlikely for the k_{add} to be rate limiting (as assumed by case 3). Furthermore, Tanaka *et al.* recently classified selectivity of various RAFT-SUMI monomer and RAFT agent pairs, categorizing maleimide and acrylate monomers with RAFT agents bearing tertiary carboxyalkyl fragmentation to be driven by the chain transfer equilibrium, thus we can assume that the kinetics of these monomer classes can be classified under case 2, where monomer addition to the R• radical, defined by k_i , is rate limiting.¹³ Therefore, we will use case 2 (equation 13) to model the kinetics of the monomers defined in this text (**Scheme 2**), where apparent rate constants (k_{app}) can be defined by equation S11.

Although these fits use only 3 to 5 data points, we emphasize that this is sufficient to estimate k_{app} values, which is further demonstrated with model polymerizations of M_{2B} and M_{2F} with CTA₂,

where more kinetic data points are taken, demonstrating little difference in obtained k_{app} values (Figure S2-S4, Table S3-S5).

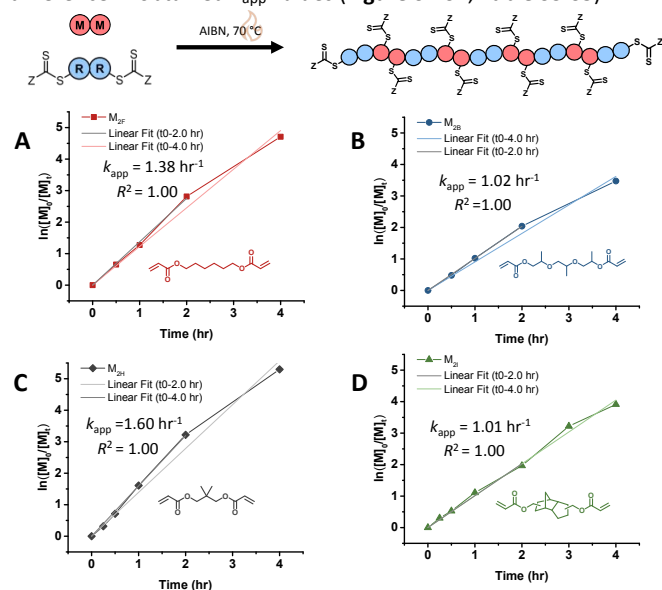


Figure 3: Kinetic analysis of RAFT step-growth for diacrylate monomers with CTA₂: (A) M_{2F}, (B) M_{2G}, (C) M_{2H}, and (D) M_{2I}.

Previously, Tanaka *et al.* varied monomer concentration for AB RAFT step-growth using monomer MCTA (Scheme 2).⁸ Conditions for both holding initiator concentration constant ($[AIBN]_0 = 0.05$ M) and holding initiator to RAFT agent ratio constant ($[MCTA]_0/[AIBN]_0 = 20$) were investigated and fitted to determine k_{app} values (Table S6-S7, Figure S5-S6). Similarly, Archer *et al.* investigated the dependence of monomer concentration for A₂ + B₂ RAFT step-growth of diacrylates by varying monomer concentration of M_{2F} polymerized with CTA₂ while either holding initiator concentration constant ($[AIBN]_0 = 0.05$ M) or holding initiator to RAFT agent ratio constant ($[CTA]_0/[AIBN]_0 = 40$) (Figures S7-S8, Tables S8-S9).¹⁰ Keeping the initial initiator concentration constant for both maleimides and acrylates displayed slight variation in k_{app} values. However, varying initiator concentration by a factor of 2 demonstrated significant changes in k_{app} values equivalent to 2^{1/2}, which is in accordance with equation 11, where R_p is dependent on $[I]^{1/2}$. These findings of R_p dependence on initiator concentration (rather than on the ratio of CTA to initiator) differs from traditional RAFT chain-growth polymerization kinetics, where the kinetics are dependent on CTA to initiator ratio as modelled by the intermediate radical termination (IRT) model.²³ This lack of retardation in RAFT step-growth polymerization is likely attributable to the rapid fragmentation of the R-group from the RAFT agent. However, as the reaction progresses, it is important to consider that the RAFT process may begin to compete with chain transfer involving the polymer backbone CTA. This competition could lead to an increased occurrence of degenerative chain transfer (or equivalent fragmentation), ultimately resulting in retardation.

Furthermore, various maleimide monomers polymerized with CTA₂ (M_{2A}, M_{2B}, M_{2C}, M_{2D}, and M_{2E}) were fitted according to case 2 to determine k_{app} (Figure 1B and 2, Table S1 and S10).^{8,9} Monomers M_{2A} and M_{2B} when polymerized demonstrate k_{app} values of approximately 2.0 hr⁻¹. Interestingly, polymerization of bis(3-ethyl-5-

methyl-4-maleimidophenyl)methane (M_{2C}) with CTA₂ displayed a slower rate compared to M_{2A} and M_{2B} ($k_{app} = 0.53$ hr⁻¹), which is consistent with literature, where *N*-aromatic maleimides with alkyl *ortho*-substituents display reduced polymerization rates.²⁴ Additionally, polymerization of 2,2-bis[4-(4-maleimidophenoxy)phenyl]propane (M_{2D}) with CTA₂ showed an increase in polymerization rate ($k_{app} = 2.68$ hr⁻¹), suggesting that *O*-phenyl substituents *para* to the maleimide ring increases polymerization rate and monomer reactivity. Lastly, 4,4-substituted phenylene bismaleimide (M_{2E}), where the maleimide units are attached to the same phenyl ring, gave rate constants (k_{app}) of approximately 1.5 hr⁻¹.

Next, RAFT step-growth polymerizations of various acrylate monomers (M_{2F}, tripropylene glycol diacrylate (M_{2G}), neopentyl glycol diacrylate (M_{2H}), and tricyclo[5.2.1.0_{2,6}]decanedimethanol diacrylate (M_{2I})) with CTA₂ were fitted using the model derived from case 2, and k_{app} values were obtained (Figure 3, Table S11). Generally, monomers M_{2F}, M_{2G}, M_{2H}, and M_{2I} display k_{app} values of around 1.00 hr⁻¹ (Figure 3, Table S11). Notably, acrylate monomers

demonstrate lower k_{app} values compared to maleimide monomers ($k_{app} = 1.0$ hr⁻¹ and 2.0 hr⁻¹, respectively), suggesting acrylate monomers demonstrate slower addition to CTA derived R• radical compared to maleimide monomers (Figures 2 and 3). Similar trends in k_{app} values for maleimide monomers and acrylate monomers is seen when investigating RAFT-SUMI kinetics of model monomers *N*-ethyl maleimide (MA) and butyl acrylate (BA) with monofunctional RAFT agent BDMAT, where $k_{app} = 0.973$ hr⁻¹ and 0.58 hr⁻¹, respectively (Figure S9-S10, Table S12).^{8,10}

Lastly, we compared the rate of polymerization for monomers M_{2B}, M_{2F}, and M_{2I} polymerized with disulfide tethered bifunctional RAFT agent, CTA_{2SS} (Figure S11, Table S13).^{10,25,26} The polymerization rate for CTA_{2SS} with M_{2B} and M_{2F} does not drastically change ($k_{app} \sim 2.0$ hr⁻¹, $k_{app} \sim 1.0$ hr⁻¹, respectively), suggesting the disulfide bond tethering the bifunctional RAFT agent does not affect the rate as the R• radical is identical for CTA₂ and CTA_{2SS}. Interestingly, silyl ether tethered diacrylate monomer (M_{2J}) when polymerized under RAFT step-growth with CTA_{2SS} shows a reduced rate ($k_{app} = 0.69$ hr⁻¹), possibly suggesting reduced monomer reactivity.

In summary, thermally initiated RAFT step-growth polymerization kinetics of maleimide and acrylate monomers with bifunctional RAFT agents with tertiary carboxyalkyl stabilized fragmentations have been successfully modelled. By analytically solving the governing equations for these polymerizations, we determined that the kinetics follows first order behavior with respect to monomer concentration. This is attributed to the rate limiting step for the investigated monomer classes being monomer addition to the R• species from RAFT agent fragmentation, characterized by the kinetic parameter k_i . Furthermore, after modelling the polymerization for a variety of maleimide and acrylate monomers, it was found that acrylate monomers exhibit lower k_{app} values compared to maleimides, which is likely due to slower monomer

addition to the R• species for acrylates compared to maleimides. Additionally, we demonstrate the $[I]^{1/2}$ dependence of R_p through fitting polymerizations conducted with varied monomer and initiator concentrations for both acrylates and maleimides.

Author Contributions

The manuscript was written through contributions of all authors.

Conflicts of interest

The authors declare the following competing financial interest(s): J.T. and W.Y. are named inventors on a patent application owned by UNC-Chapel Hill (PCT/US2022/042087) which laid the foundation for this work. Dr. You is also a co-founder of Delgen Biosciences, a startup company that has licensed this UNC patent application.

Acknowledgements

This work was financially supported by the National Science Foundation (NSF) under Award CHE-2108670. This material is based upon work supported by the National Science Foundation Graduate Research Fellowship Program under Grant No. (NSF DGE-2439854). Bruker AVANCE III Nanobay 400 MHz NMR Spectrometer was supported by NSF under Grant No. CHE-0922858, and Bruker NEO 600 MHz NMR spectrometer was supported by NSF under Grant No. CHE-1828183. Authors thank Dr. Marc A. ter Horst from University of North Carolina's Department of Chemistry NMR Core Laboratory for the use of the NMR spectrometers.

Notes and references

1. S. Perrier, *Macromolecules*, 2017, **50**, 7433-7447.
2. J. Chiefari, Y. K. Chong, F. Ercole, J. Krstina, J. Jeffery, T. P. T. Le, R. T. A. Mayadunne, G. F. Meijs, C. L. Moad, G. Moad, E. Rizzardo and S. H. Thang, *Macromolecules*, 1998, **31**, 5559-5562.
3. C. L. Moad and G. Moad, *Chemistry Teacher International*, 2021, **3**, 3-17.
4. N. Corrigan, K. Jung, G. Moad, C. J. Hawker, K. Matyjaszewski and C. Boyer, *Progress in Polymer Science*, 2020, **111**.
5. J. Zhang, B. Farias-Mancilla, I. Kulai, S. Hoepfener, B. Lonetti, S. Prevost, J. Ulbrich, M. Destarac, O. Colombani, U. S. Schubert, C. Guerrero-Sanchez and S. Harriison, *Angew Chem Int Ed Engl*, 2021, **60**, 4925-4930.
6. Y. Zhang, Y. Tang, J. Zhang and S. Harriison, *ACS Macro Lett*, 2021, **10**, 1346-1352.
7. L. Billiet, D. Fournier and F. Du Prez, *Polymer*, 2009, **50**, 3877-3886.
8. J. Tanaka, N. E. Archer, M. J. Grant and W. You, *J. Am. Chem. Soc.*, 2021, **143**, 15918-15923.
9. P. Boeck, N. Archer, J. Tanaka and W. You, *Polym. Chem.*, 2022, **13**, 2589-2594.
10. N. E. Archer, P. T. Boeck, Y. Ajirniar, J. Tanaka and W. You, *ACS Macro Letters*, 2022, **11**, 1079-1084.
11. S. M. Clouthier, J. Tanaka and W. You, *Polym. Chem.*, 2022, **13**, 6114-6119.
12. P. T. Boeck, J. Tanaka, W. You, B. S. Sumerlin and A. S. Veige, *Polym. Chem.*, 2023, **14**, 2592-2598.
13. J. Tanaka, J. Li, S. M. Clouthier and W. You, *Chem. Commun.*, 2023, **59**, 8168-8198.
14. R. Wei, T. Tiso, J. Bertling, K. O'Connor, L. M. Blank and U. T. Bornscheuer, *Nature Catalysis*, 2020, **3**, 867-871.
15. R. Liu, L. Zhang, Z. Huang and J. Xu, *Polymer Chemistry*, 2020, **11**, 4557-4567.
16. S. Houshyar, D. J. Keddie, G. Moad, R. J. Mulder, S. Saubern and J. Tsanaktisidis, *Polymer Chemistry*, 2012, **3**.
17. J. Xu, *Macromolecules*, 2019, **52**, 9068-9093.
18. L. Zhang, R. Liu, Z. Huang and J. Xu, *Polymer Chemistry*, 2021, **12**, 581-593.
19. N. B. Cramer, T. Davies, A. K. O'Brien and C. N. Bowman, *Macromolecules*, 2003, **36**, 4631-4636.
20. N. B. Cramer, S. K. Reddy, A. K. O'Brien and C. N. Bowman, *Macromolecules*, 2003, **36**, 7964-7969.
21. S. K. Reddy, N. B. Cramer and C. N. Bowman, *Macromolecules*, 2006, **39**, 3673-3680.
22. G. Moad, *Progress in Polymer Science*, 2019, **88**, 130-188.
23. K. G. E. Bradford, L. M. Petit, R. Whitfield, A. Anastasaki, C. Barner-Kowollik and D. Konkolewicz, *J Am Chem Soc*, 2021, **143**, 17769-17777.
24. A. Matsumoto, T. Kubota and T. Otsu, *Macromolecules*, 1990, **23**, 4508-4513.
25. O. R. Courtney, S. M. Clouthier, S. Perrier, J. Tanaka and W. You, *ACS Macro Lett*, 2023, **12**, 1306-1310.
26. S. M. Clouthier, J. Li, J. Tanaka and W. You, *Polymer Chemistry*, 2024, **15**, 17-21.

- The data supporting this article have been included as part of the Supplementary Information.